Radiation-Hydrodynamic multi-species escape from Hot Jupiters

Matthäus Schulik[1], Richard Booth[1], James Owen[1]
[1]*Imperial College London, Exhibition Rd, South Kensington, London SW7 2BX, United Kingdom*

Abstract

Photoevaporative models are an important tool for helping to understand the radius distribution of exoplanets. So far, those models have often focused on the escape of H/He mixtures, neglecting coupled escape with heavier species, or assumed a fixed hierarchy of major and minor species. In this work, we relax those assumptions by using a truly multi-species simulation framework, including radiation transport and friction. We present a set of tentative results aiming at understanding the behaviour of solutions we find for Hot Jupiter exoplanets. This will open the path for the investigation of other classes of exoplanets in the near-future.

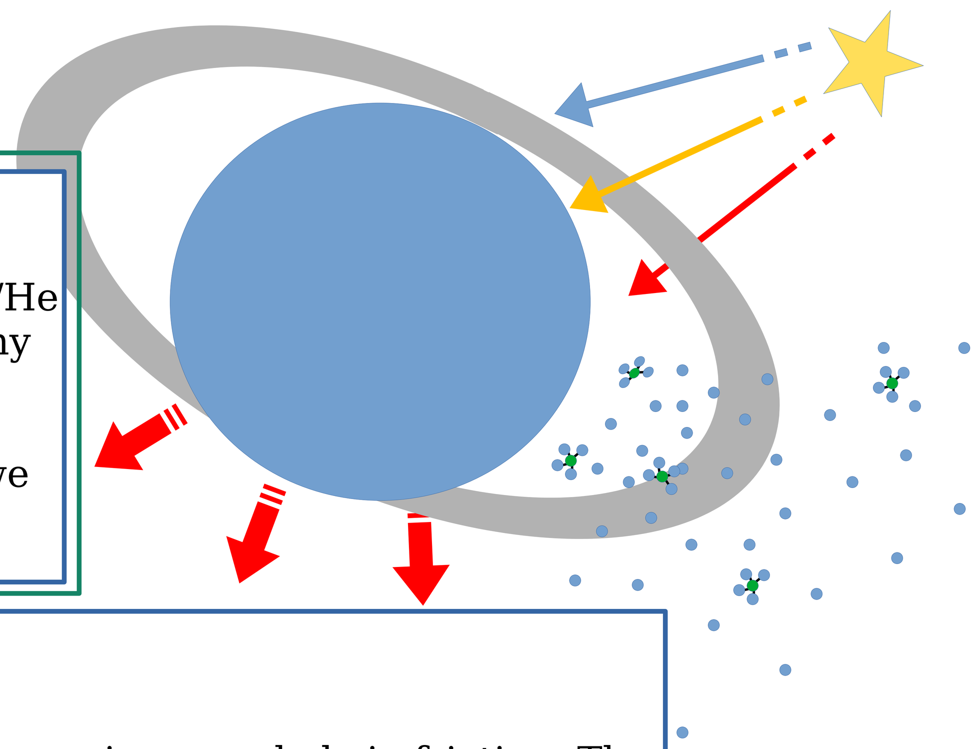

Project goal

We aim to study the transition to metal-dominated atmospheres in Sub-Neptune exoplanets via coupled hydrogen-metal hydrodynamic escape.
As our model adds thermal heating and cooling as well as friction between individual species, we benchmark the physics first against established Hot Jupiter models. We focus on comparing models of Hot Jupiters with m=224 m_e and d=0.05 AU around a G0-type star and leave the Sub-Neptune exoplanets for a later project part.

Methods

* We solve the hydrodynamic equations for multiple species, coupled via friction. The fluids can radiate in several broad bands on a static, one-dimensional spherically-symmetric grid.

The physics modules are solved operator-split according to the appropriate methods:
* Hydrodynamics: HLLC (Toro 2009)+Well-balancing (Käppeli&Mishra 2016)
* Friction between species: Implicit scheme by Benitez-Llambay+(2019)
* Radiative transport: Multi-band flux-limited diffusion Inspired by Commercon+(2011), Vaytet+(2012) and Bitsch+(2013)/Lega+(2014).

1. Thermally-driven winds

We first investigate the impact of thermal solar irradiation and thermal cooling on the escape of hydrogen coupled to methane. No XUV luminosity is irradiated. The appearance of temperature minima is controlled by the magnitude of the opacity κ_{star} to solar irradiation (Guillot 2010).

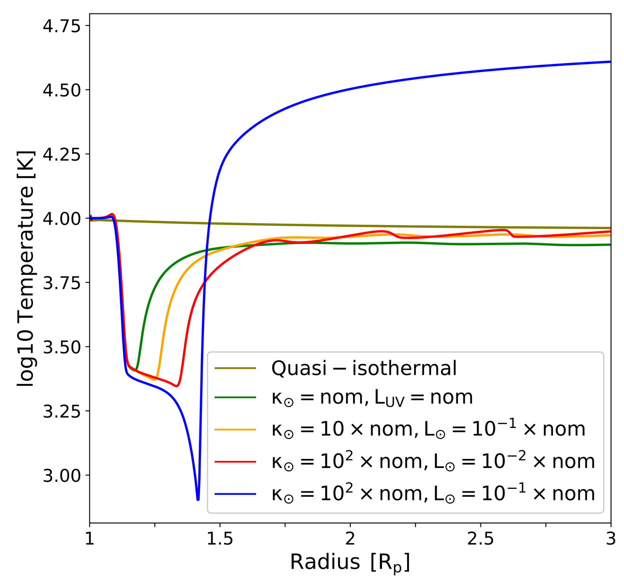

Fig. 1: Influence of atmospheric temperature structures

* In a two-species model, we keep the thermospheric temperature approx. constant by keeping $L_{star} \times \kappa_{star}$ constant.

* Additionally, one simulation is added with extremely high thermospheric temperature, but constant stratospheric temperature.

* Those runs are compared to an isothermal model.

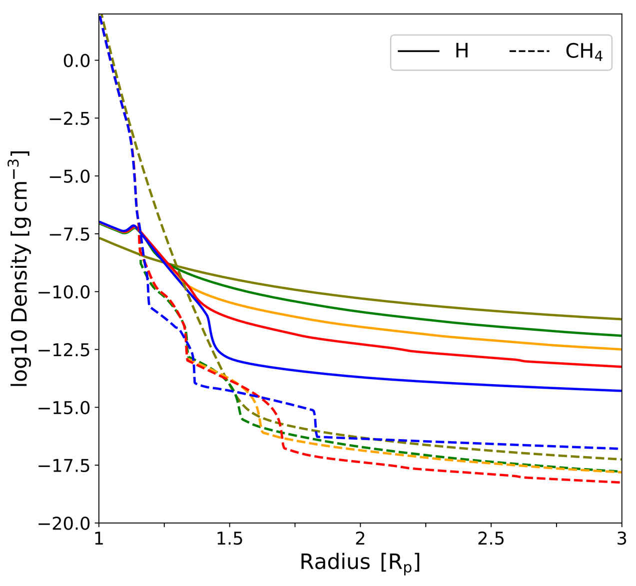

Fig.2: Transport of a secondary atmospheric species

* Simulations start with adiabatic profiles for both species. At r<1.3 r_P Methane is the dominant species, above it is hydrogen.

* Hydrogen readily escapes at 10.000K temperature and is coupled via the Schunk & Nagy (1980) collision coefficients to Methane, which would otherwise not escape.

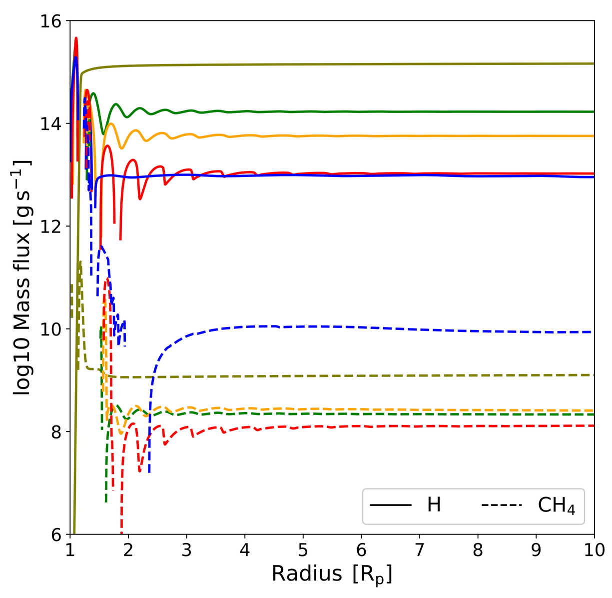

Fig. 3: Mass-loss of primary and secondary species:

* Hydrogen mass-loss reduces linearly with the width of the temperature minimum

* Increasing the thermospheric temperatures does not affect the hydrogen escape rates. This can be understood as 'cold trap' effect of the temperature minimum.

* The escape rates of the secondary species are sensitive to the thermospheric temperature (see orange vs. green and blue curves). This is caused by the hot thermospheric hydrogen escaping very fast and hence dragging methane efficiently.

Conclusion: **The temperature structure between the mass reservoir of potentially escaping species and the sonic point does matter. A most interesting finding is the different sensitivity of the two species to the thermospheric temperature.**

2. Transition to metal-dominated atmospheres

Our nominal radiative simulation experiences strong hydrogen loss leading to its depletion around the τ_{VIS}=1-surface. Methane takes over as dominant atmospheric species at those altitudes, while a low-lying methane reservoir remains. Here we briefly characterize this process.

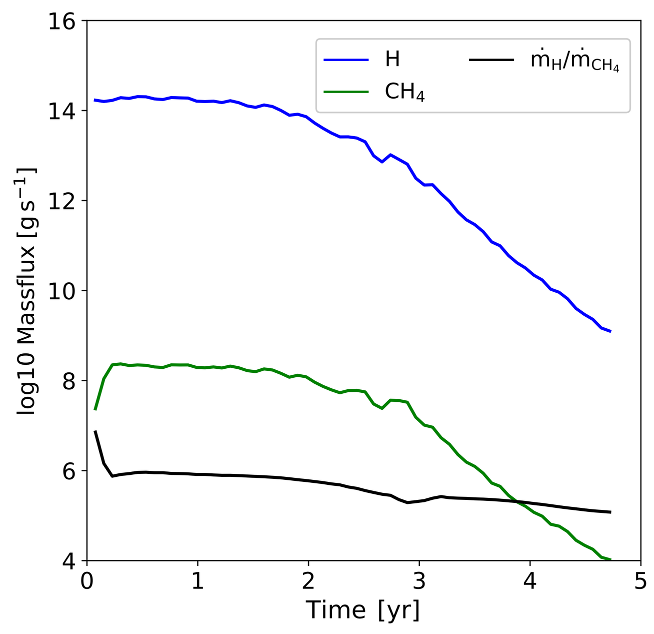

Fig. 4: Decrease of Hydrogen and methane mass-loss with time, as the hydrogen reservoir is depleted.

* Initially, both escape rates remain approx. constant, as long as the hydrogen reservoir (m_H=10^{-5} m_e) is not significantly affected by escape

* Methane escape rates co-evolve with the hydrogen escape rates, but their ratio favours more and more methane escape.

* The flux ratio is proportional to the density ratio in the outflow. Hence, while less hydrogen escapes, it remains to be seen whether a non-zero hydrogen mixing ratio remains in the final state of the planet.

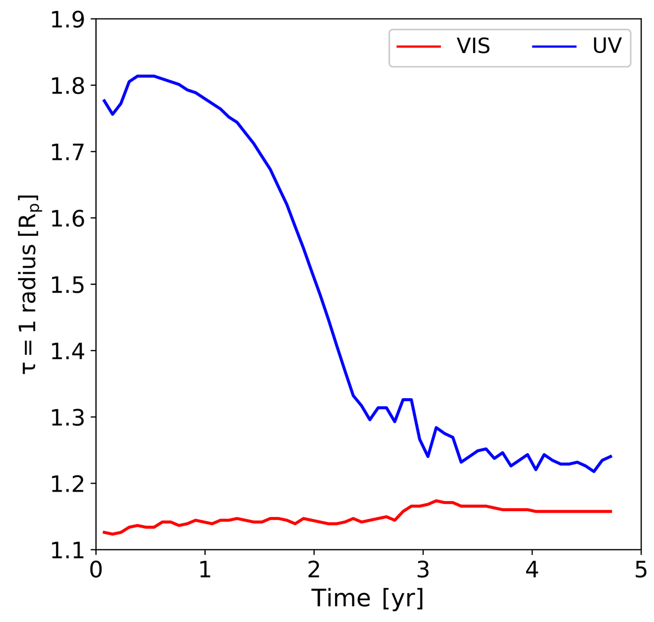

Fig. 5: Evolution of UV and visible τ=1 radii with time

* The main absorber in the UV is hydrogen, which once depleted shrinks the planetary UV surface.

* The slight increase in visible τ=1 radius, is a result of the coupled species dynamics: As hydrogen mass flux shuts down, methane cannot escape from the upper atmosphere anymore and accumulates there.
This effect starts to reverse again, as methane drops into the lower atmosphere.

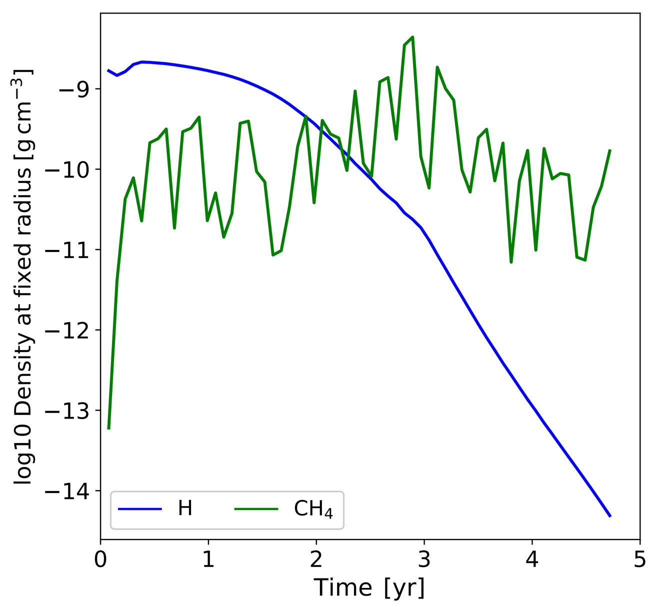

Fig. 6: Transition to a metal-dominated atmosphere

* At a fixed radius of 1.25 RP, just above the visible τ=1 radius, we plot the densities of both species.

* The hydrogen depletion is evident, as well as the reason for the increase in visible tau=1 altitude.

* Lower altitudes deplete even faster of hydrogen, as the relative abundance of methane there is higher.

Conclusion: **While those first results successfully show a proof-of-concept transition, longer simulation times, or a snapshot appproach e.g. coupled with MESA, will be needed to decide the final mixing ratio of hydrogen in metal-dominated atmospheres.**

3. Literature comparison

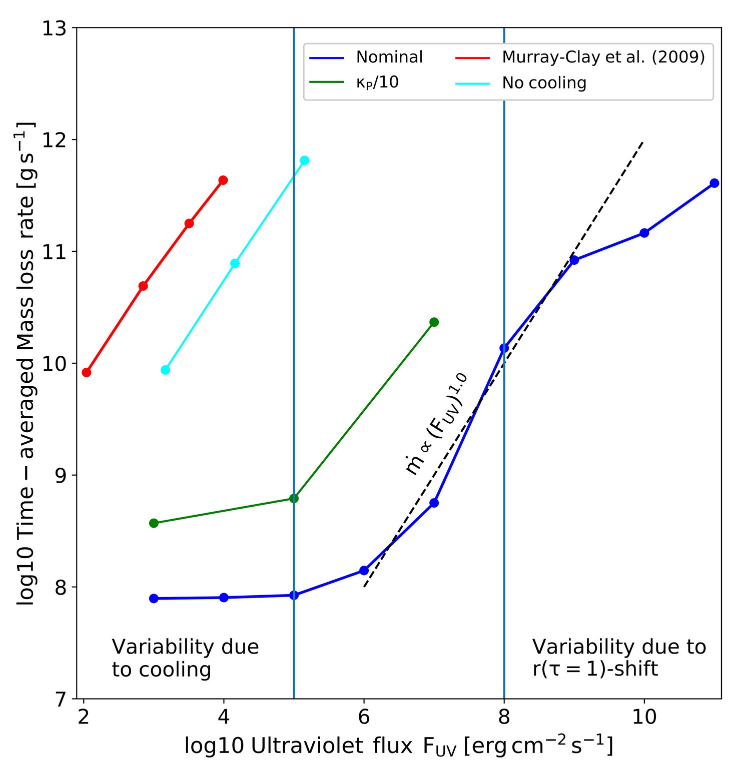

Fig. 7: Hydrogen-only mass-loss rates with our full modell

* Including thermal and UV heating and thermal cooling via Freedman+(2014) and Malygin+(2014) opacities, reduces temperatures and hence escape rates drop drastically (blue curve), with a minimum escape rate given by thermal irradiation.
* Two variability regimes exist. At low FUV, individual gas pockets cool, and loose pressure support, falling back, leading to intermittent escape. At high FUV, the escaping mass is enough to change the UV absorption altitude.

* As important check, we disable radiation transport which results as in similar physics as in Murray-Clay+(2009) (cyan curve)

* Another test with reduced Planck-opacities mimicks a molecule-depleted upper atmosphere, which increases escape rates due to less efficient thermal cooling (green curve).

Conclusion:
Including thermal cooling can shut down escape. However, the tabulated opacities assume typically solar atom/molecule mixes which should be reduced or destroyed in UV-irradiated heterospheres. Hence our nominal results probably underestimate escape as they represent the maximum possible cooling rate.

4. Outlook

* In the near-future we work to include the effects of photoionization via C²-ray by Mellema+(2006). This will result in models that are entirely comparable to the literature values and should resolve remaining discrepancies in adiabatic simulations.

* Individual species will need dedicated Planck and Rosseland mean-opacities in order to correctly compute temperature structures of mixed atmospheres

* Sub-Neptunes and Super-Earths are the natural objects to study next.

References

Benitez-Llambay+(2019),	doi:10.3847/1538-4365/ab0a0e
Bitsch+(2013),	doi:10.1051/0004-6361/201220159
Commercon+(2011),	doi:10.1051/0004-6361/201015880
Freedman+(2014),	doi:10.1088/0067-0049/214/2/25
Guillot (2010)	doi:10.1051/0004-6361/200913396
Käppeli / Mishra 2016,	doi:10.1051/0004-6361/201527815
Lega+(2014),	doi:10.1093/mnras/stu304
Malygin+(2014),	doi:10.1051/0004-6361/201423768
Mellema+(2006),	doi:10.1016/j.newast.2005.09.004
Murray-Clay+(2009),	doi:10.1088/0004-637X/693/1/23
Schunk & Nagy (1980),	doi:10.1029/RG018i004p00813
Toro (2009),	doi:10.1007/b79761
Vaytet+(2011),	doi:10.1051/0004-6361/201219427